Article

Not peer-reviewed version

Clarifying the Dominant Role of Crystallinity and Molecular Orientation in Differently Processed Thin Films Regioregular poly(3-Hexylthiophene)

Kumar Vivek Gaurav *, Harshita Rai, Kshitij RB Singh, Shubham Sharma, Yoshito Ando, SHYAM S. PANDEY *

Posted Date: 29 April 2024

doi: 10.20944/preprints202404.1914.v1

Keywords: Regioregular poly(3-hexylthiophene); organic field-effect transistors; thin films; crystallinity; orientation; unidirectional floating film transfer

 doi:10.20944/preprints202404.1914.v1

Article

Clarifying the Dominant Role of Crystallinity and Molecular Orientation in differently Processed Thin Films Regioregular Poly(3-hexylthiophene)

Kumar Vivek Gaurav *, Harshita Rai, Kshitij RB Singh, Shubham Sharma, Yoshito Ando and Shyam S. Pandey *

Graduate School of Life Science and Systems Engineering, Kyushu Institute of Technology, Kitakyushu, Fukuoka, 808-0196 Japan

* Correspondence: kvgaurav2010@gmail.com (K.V.G), shyam@life.kyutech.ac.jp (S.S.P)

Abstract: Conjugated polymers (CPs) offer potentials for sustainable semiconductor devices due to their low cost, and inherent molecular self-assembly. Enhanced crystallinity and molecular orientation in thin films of solution-processable CPs have significantly improved organic electronic device performance. In this work, three methods namely spin-coating, dip-coating, and unidirectional floating-film transfer method (UFTM) were utilized with their parametric optimization for fabricating RR-P3HT films. These films were then utilized for their characterization via optical and microstructural analysis to elucidate dominant roles of molecular orientation, and crystallinity in controlling charge transport in organic field-effect transistors (OFETs). OFETs fabricated by RR-P3HT thin films using spin-coating and dip-coating displayed field-effect mobility (μ) of 8.0 × 10^{-4} $cm^2V^{-1}s^{-1}$ and 1.3 × 10^{-3} $cm^2V^{-1}s^{-1}$, respectively. This two-time enhancement in (μ for dip-coated films was attributed to its enhanced crystallinity. Interestingly, UFTM films based OFETs demonstrated μ of 7.0 × 10^{-2} $cm^2V^{-1}s^{-1}$, >100 times increment as compared to its spin-coated counterpart This superior device performance is attributed to synergistic influence of higher crystallinity and molecular orientation. Since the crystallinity of dip-coated and UFTM-thin films are similar ~50 times improved μ of UFTM thin films suggest a dominant role of molecular orientation as compared to crystallinity in controlling the charge transport.

Keywords: Regioregular poly(3-hexylthiophene); organic field-effect transistors; thin films; crystallinity; orientation; unidirectional floating film transfer

1. Introduction

Semiconductor technology has developed and evolved rapidly, which has enabled the fabrication of miniaturized and efficient electronic devices. Further, from the invention of transistors (the 1950s) to today's scenario of integrating billions of transistors on a single chip; semiconductor technology has revolutionized electronic devices [1]. Now time demands the development of sustainable semiconductor devices owing to the paradigm shift from hard and brittle to soft and flexible. Thanks to the discovery of organic conjugated polymers having the capability of low-cost fabrication, light-weight, flexible and natural tendency of molecular self-assembly, that offers various applications in the field of organic electronic devices [2], such as organic field-effect transistors (OFETs) [3], organic light emitting diodes [4,5], memristors [6], organic solar cells [7], etc. Moreover, OFETs can be developed as a promising frontier, utilizing organic materials instead of traditional semiconductors, owing to their potential advantages such as flexibility, low-cost manufacturing, and compatibility with unconventional substrates, paving the way for flexible electronics for developing wearable devices. However, challenges remain in achieving comparable performance to conventional semiconductor technologies, driving ongoing research and development in this exciting field.

To address these challenges, there is a need to understand and study various components involved in the fabrication of organic electronic devices, as it is a fast-growing area and the fabrication

 doi:10.20944/preprints202404.1914.v1

of these electronic devices, organic semiconductors is the pillar. Among the various components involved in fabricating organic electronic devices utilizing solution-processable conjugated polymers (CPs), thin film fabrication is the most important [8–11], as the device characteristics are greatly influenced by the thin film morphology of the CP layer [12–14]. For practical applications, managing the cost and performance of these OFETs are the primary challenges. The performance of these devices depends on CPs and the nature of thin films. Further, various methods of thin film fabrication can be opted, according to the device's requirement, as OFETs are planar devices, a homogenous and aligned thin film in the direction of the channel with an edge-on orientation is preferred for the better device performance. There are several methods for thin film fabrication, such as bar coating [15], mechanical rubbing [16], and friction transfer [17], but they have issues like mechanical damage or face-on orientation, which are not suitable for planar devices and cannot be used for multilayer fabrication of the active organic semiconducting layer based on pure solution based thin film fabrication approaches. The most widely used spin coating technique though results in a thin film with crystalline domains distributed in an amorphous sea of polymeric chains resulting in hampered device performance [18,19]. Therefore, methods involving increased molecular self-assembly and better molecular alignment are highly required. To circumvent these issues, thin film fabrication techniques such as dip coating [20] can be used, which can not only harness the enhanced molecular self-assembly of CPs but also solve the huge material wastage in the case of spin-coating. At the same time, the unidirectional floating-film transfer method (UFTM) [21], developed and improvised by our research group provides large area, uniform, anisotropic, and edge-on oriented thin film with the least material wastage. To access the quality of thin films fabricated by various methods in depth; optical, microstructural and electrical characterizations are very crucial.

Owing to the CPs' quasi-one-dimensional nature, many researchers have investigated their backbone orientation and self-assembly to enhance the optoelectronic properties of the devices [22,23]. Alkyl-substituted CPs exhibit good solubility in common halogenated solvents, which are often used for the fabrication of thin films and their utilization of organic electronic devices [24,25]. There are reports for the fabrication of thin films using different thin film fabrication methods results are scattered in terms of the CPs and method of film fabrication under investigation. Since both the factors such as the nature of the CP and the method of the film fabrication have a profound influence on the morphology, crystallinity and orientation in the fabricated thin films, it is difficult to pinpoint the roles of the thin film crystallinity and molecular orientation on the charge transport in general and device performance in particular. Therefore, in this present work, regioregular poly(3-hexylthiophene) (RR-P3HT) was used as a solution-processable representative organic semiconductor to fabricate OFETs, where thin films of this polymer were fabricated by different methods such as UFTM, dip-coating, and spin coating. Various parameters were first optimized under each type of film fabrication method followed by their optical and microstructural characterizations. Finally, OFETs were fabricated to analyze the implications of molecular orientation, uniformity and crystallinity on the charge transport, and device performance.

2. Materials and Methods

2.1. Materials

An electronic grade RR-P3HT with the molecular structure shown in Figure 1(a) has been procured from Lisicon, Merck, USA and used as a representative solution processable CP for this work. All the solvents, used for cleaning of the substrate including hexane, acetone, methanol, and toluene were acquired from Fujifilm Wako, Japan. Some other solvents, used in the process, such as super-dehydrated chloroform, octadecyltrichlorosilane (OTS) and hexamethyldisilane (HMDS) were procured from Sigma Aldrich, USA. Super-dehydrated chloroform was used to make the RR-P3HT solution of varying concentrations. Ethylene glycol (Eg) and Glycerol (Gl) were purchased from Fujifilm Wako, Japan and were used to prepare viscous liquid substrates of varying viscosities. CYTOP (CTL-809 M) and its diluting solvent (CTSOLV 180) were purchased from AGC, Japan and used as it is without any further purification. Chemicals such as octadecyl trichlorosilane (OTS), hexamethyldisilazane (HMDS) and CYTOP a fluoropolymer were used as surface modifiers on the

 doi:10.20944/preprints202404.1914.v1

glass and Si/SiO_2 substrates before thin film fabrication of RR-P3HT under different film fabrication methods.

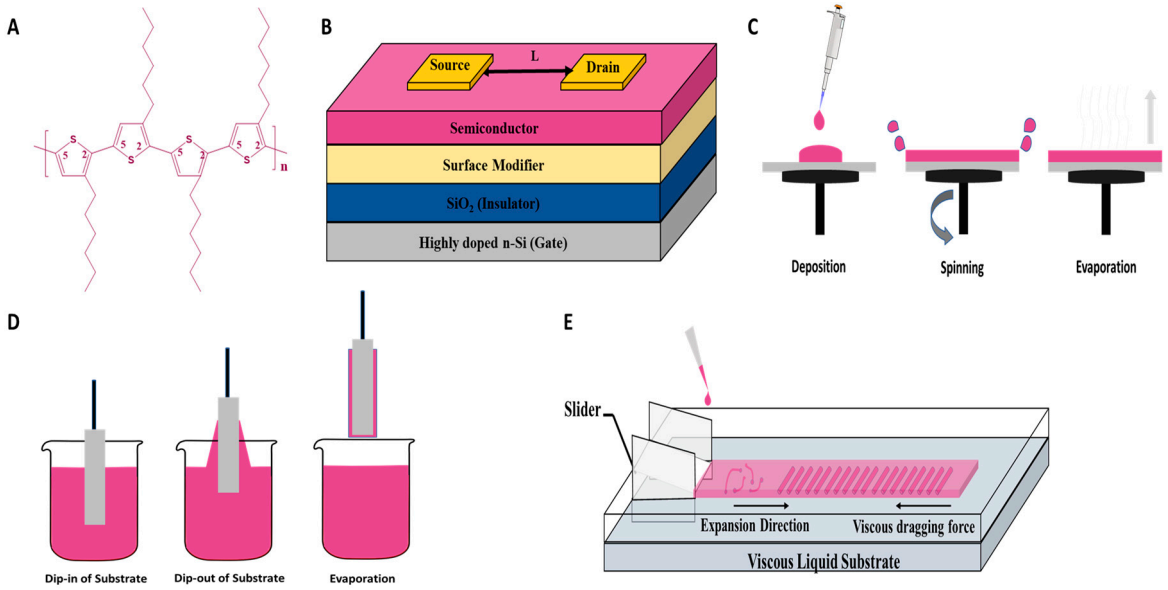

Figure 1. A) Structure of RR-P3HT; B) Schematic representations for OFET device architecture, C) Spin coating, D) Dip coating, and E) UFTM.

2.2. Thin film and Device Fabrication

For the fabrication of thin films, three different techniques such as dip-coating, spin coating and UFTM have been used in this study: For the optimization of the fabrication conditions, thin films were fabricated on glass substrates and finally, devices were fabricated under optimized conditions on the Si/SiO_2 (300nm) substrates for the investigation of charge transport by OFET fabrication. Substrates were cleaned by hexane wiping followed by sonication in acetone, methanol, and chloroform for 10 minutes each. After sonication, the substrates were subjected to different surface treatments such as UV-Ozone, HMDS, OTS and CYTOP, which were used to modify the surface of the substrates. The cleaned substrates were subjected to UV ozone for 10 minutes before being used for film fabrication. For HMDS surface treatment, the 20% HMDS solution was prepared in super-dehydrated hexane at room temperature followed by dipping of the substrates in this solution for 10 minutes at 45°C and its cleaning by sonication in hexane for 10 minutes. Finally, substrates were annealed at 100°C for 30 minutes to remove any residual solvents before the fabrication of thin films of RR-P3HT. OTS surface treatment was conducted by putting the substrates into 20 mM OTS solution in toluene for 36 hours at room temperature to form a self-assembled monolayer (SAM). These substrates were then sonicated in toluene for 10 minutes and annealed at 180°C for 30 minutes. In the case of using CYTOP as a surface modifier, CYTOP solution (1:3, v/v) was prepared by its dilution using CT-SOLV solvent, which was spin-coated on the substrates for 60 seconds at 2000 rpm, followed by annealing in an argon atmosphere at 180°C for 1 hour. Optical, surface and microstructural characterizations were performed after casting the thin films of RR-P3HT using different techniques onto the modified glass substrate as discussed above followed by annealing at 120°C. The OFET fabrication was done in bottom gate top contact (BGTC) device architecture on the Si/SiO_2 substrates as shown in Figure 1(B). After casting the thin films on surface modified Si/SiO_2 substrate, annealing was performed at 120°C. Finally, nickel shadow masks were used to pattern source/drain electrodes using thermal vapor deposition of gold under a 10^{-6} Torr.

2.2.1. Spin Coating

Spin coating is the simplest and the most widely used technique to fabricate thin films of the solution processable materials. In this method, a small amount of material is applied onto a desired

 doi:10.20944/preprints202404.1914.v1

substrate followed by its spreading throughout the substrate and spinning at a defined speed using a spin coater (ACT-220 DII) as shown in Figure 1(C). Optimization of film fabricated on the various surface-treated substrates was performed by varying concentration and spinning speed. The concentration range was varied between 0.1 – 1 % (w/v) and the spinning speed was varied between 1000 – 3500 rpm. Finally, the OFET device was fabricated under optimized conditions of 0.5% (w/v) of RR-P3HT in super dehydrated chloroform solution at 3500 rpm for 40 s on an HMDS-treated Si/SiO_2 substrate.

2.2.2. Dip Coating

In this method, the cleaned and surface-modified substrates were vertically dipped in the desired solution, held for some time, and then lifted at a predefined speed as shown in Figure 1(D). using a dip-coater (Nano Dip-Coater, ND-0407, SDI Japan). The concentration of RR-P3HT solution was varied from 0.05 to 1% (w/v), whereas the lifting speed was varied between 20 to 200 μms^{-1} for the optimization of the film quality utilizing various surface-modified substrates. After optimization, OFETs were fabricated by dip-coated RR-P3HT thin films utilizing the optimum 0.1% (w/v) concentration, 20 μms^{-1} of lifting speed to the HMDS-treated Si/SiO_2 substrate.

2.2.3. Unidirectional Floating Film Transfer Method

In this method, a very small amount (~10 µL) of the RR-P3HT solution in chloroform was dropped onto an orthogonal viscous liquid substrate consisting of ethylene glycol (EG) and glycerol (GL) as shown in Figure 1(E). UFTM imparts not only large area uniform thin films but also these films are oriented perpendicular to the spreading direction of the floating film. The extent of the orientation/alignment under UFTM can be controlled by optimizing the film formation parameters such as concentration of the polymer solution, viscosity of the liquid substrates and temperature. In this work, efforts were directed to study the impact of different surface treatment conditions of the substrates on UFTM-processed thin films and varied the concentration of RR-P3HT polymer solution from 1.5 – 7% (w/v). Oriented thin films under optimized conditions of 4% (w/v) polymer concentration, EG: GL liquid substrate (3:1) at 50°C on HMDS treated Si/SiO_2 (300 nm) substrate was used for the OFET fabrication and investigation of charge transport.

2.3. Thin Film and Device Characterizations

2.3.1. Optical and Microstructural Characterizations

The UV-vis-NIR spectrophotometer (Jasco V-570) was used to measure the electronic absorption spectra of the spin-coated, dip-coated, and UFTM-processed thin films. Since UFTM-processed thin films were oriented and anisotropic, to measure the extent of optical anisotropy, the Glan Thompson polarizing prism was used during the measurement of the absorption spectrum. The polarizer was positioned between the incident light source and the UFTM film, and its rotation angle controlled the polarization direction of the incident beam. This allowed for the measurement of the polarized electronic absorption spectrum, specifically in the parallel (∥) and perpendicular (⊥) directions of the film orientation. Further investigation of optical anisotropy in oriented thin films prepared by UFTM was conducted in terms of dichroic ratio (DR), as determined by Eq. (1).

$$\boldsymbol{DR = \frac{Maximum\ Absorption\ \text{at}(\lambda_{max}\ ||)}{Absorption\ \perp\ \text{at}\ \lambda_{max}\ ||)}} \quad (1)$$

For microstructural characterizations, the thin films prepared on clean Si substrates were subjected to X-ray diffraction (XRD) and grazing incidence X-ray diffraction (GIXD) measurements. The Cu-Kα radiation source-embedded with Rigaku X-ray diffractometer was utilized to perform out-of-plane XRD measurements. The X-rays incident on the sample experience a total external reflection when their index of refraction is less than unity. Additionally, the grazing incidence angle (ω) with the thin-film surface is smaller than the critical angle (ω_c) (i.e., $\omega<\omega_c$). The sample and detector were rotated at angles of φ and $2\theta_\chi$, respectively, for the in-plane GIXD measurement. In

 doi:10.20944/preprints202404.1914.v1

addition, the angle between the film expansion during UFTM, spin coating, and dip coating the scattering vector (χ) was fixed at approximately 0 or 90° to study anisotropy in the films. In contrast, the X-ray source and detector were rotated at angles of θ and 2θ, respectively, from the sample surface for the out-of-plane XRD measurements.

2.3.2. Contact Angle Measurement

Contact angle measurements are used to study the wettability of the substrate when treated with different surface modifiers. Intermolecular interactions between the liquid and the solid surface cause the contact between them to occur, which is referred to as "wetting" and the angle at which a liquid/vapor interface meets a solid surface is known as the contact angle, which describes the degree of wetting [26]. Hence, for contact angle measurement firstly, the substrates were cleaned with sonication in acetone for 10 minutes and surface modification techniques such as UV-Ozone, HMDS, OTS and CYTOP were done followed by the contact angle measurement using Kyowa Interface Science Corporation Ltd. machine (Model No: DMs-401). For this measurement, a 10 µl droplet of DI water was dropped onto the untreated and treated substrates and the contact angle was measured in degrees, which was later used to determine the nature of surface-treated substrates.

2.3.3. Electrical Characterizations

Charge transport was investigated by fabricating OFETs in the BGTC device architecture as per the conditions described in section 2.2. A highly doped Si substrate and a 300 nm thermally grown SiO_2 layer were utilized as gate and gate oxide, respectively, to fabricate OFETs having an aerial capacitance of C_i=10 nF cm^{-2}. After the fabrication of OFET on to Si/SiO_2 substrate, electrical characterizations in terms of output and transfer characteristics were performed using a computer-controlled two-channel source measurement unit (Keithley-2612) under 10^{-3} Torr.

3. Results

3.1. Contact Angle Goniometry

Several studies have shown that modifying the dielectric surface helps to improve the quality of organic semiconductor film onto the dielectric surface, which in turn particularly enhances the electrical performance. Zan and Chou [27] reported that SAMs of surface modifiers affect the surface energy of the substrate improving the quality of the thin films. We have used contact angle measurement to probe the effect of various interfacial layers of the surface modifiers on the substrate. Figure 2 shows the contact angle on the treated and untreated glass substrates. The contact angle on a bare glass substrate was measured to be 54.8° indicating its hydrophilic nature. Surface modifications of the glass substrate using HMDS, OTS and CYTOP, the contact angle increased to 86.4°, 108.9°, and 114.7°, respectively, suggesting that hydrophobicity of the glass surface increases in the order CYTOP>OTS>HMDS. Lim et al. [28] reported that the contact angle with respect to the substrate increases after treatment with HMDS and OTS, indicating that the surface energy of the substrate decreases after the treatment. However, after being subjected to UV-Ozone, the contact angle decreases to 36.5° indicating an increase in the hydrophilicity of the substrate. The theoretical description of contact arises from the consideration of thermodynamic equilibrium between the three phases: the liquid phase of the droplet, the solid phase of the substrate, and the gas/vapor phase of the ambient [29]. For flat surfaces, if the surface is hydrophilic, the contact angle will be less than 90°, and the more it is towards zero degrees, the more strongly hydrophilic the solid substrate is. Moreover, if the solid surface is hydrophobic, the contact angle will be more than 90° [30]. Hence, in our case, OTS and CYTOP depict hydrophobicity, whereas, HMDS shows a relatively less hydrophilic nature as compared to UV-ozone surface treatment.

 doi:10.20944/preprints202404.1914.v1

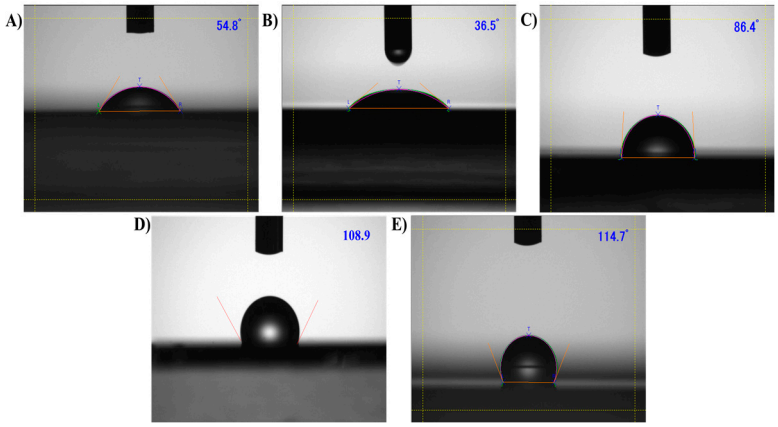

Figure 2. Contact angle of the glass substrate surface A) untreated, and treated UV-Ozone treated (B), HMDS (C), OTS (D) and CYTOP (E).

3.2. Optimization of Thin Film Fabrication

3.2.1. Spin-Coated Thin Films

Surface treatments such as HMDS, OTS, UV-Ozone and CYTOP were performed onto the cleaned glass substrate before spin coating of the RR-P3HT thin films. To understand the impact of surface modification, electronic absorption spectra were recorded (see Figure S1A, Supporting Information) and it was found that although there was a change in the peak absorbance values, there was almost no change in the positioning of the peaks, which was discernible from the normalized absorption spectra as shown in Figure 3(A). It can be seen from this figure that there was the presence of a dominant peak at 550 nm ($A_{0\text{-}1}$) corresponding to interchain interactions between the polymeric chains of the P3HT. At the same time, two shoulders one of lower energy appearing at 500 nm ($A_{0\text{-}2}$) and another at 600 nm ($A_{0\text{-}0}$) associated with the π-π^* electronic transition aggregation behavior of the polymeric chains [31,32]). It is worth mentioning that it was not possible to spin coat RR-P3HT thin film on CYTOP-treated glass substrate owing to its extremely high hydrophobic nature (Fig. S1C. Please remove Figure S1B). Considering the normalized absorption spectra RR-P3HT on HMDS and OTS-treated glass substrates, which are almost similar (Figure 1A) and uniformity of the fabricated thin films (Fig. S1C), it could be concluded that both of the surface treatments are suitable for spin coating. The spinning speed and concentration of the solution under spin-coating play a dominant in controlling the uniformity and morphology of the fabricated thin films. Spinning speed is an important factor, which not only affects the thickness but also the quality of the fabricated thin films. Therefore, it is important to optimize the effects of spinning speed, which varied from 1000 – 3500 rpm, keeping other variable parameters such as the nature of the substrate surface, and polymer concentration to be fixed. Electronic absorption spectra as shown in Figure 3(B) reveal that the thickness of the film increases by decreasing the spinning speed and there was about 1.5 times increase in the thickness of RR-P3HT thin films upon a decrease in the spinning speed from 3500 rpm to 1000 rpm [29]. In the present work, the spinning speed of 3500 rpm was used for OFET fabrication since thinner films are preferred for planar charge transport because uniformity and consistency of the film begin to get affected as we move towards lower spinning speeds [29].

 doi:10.20944/preprints202404.1914.v1

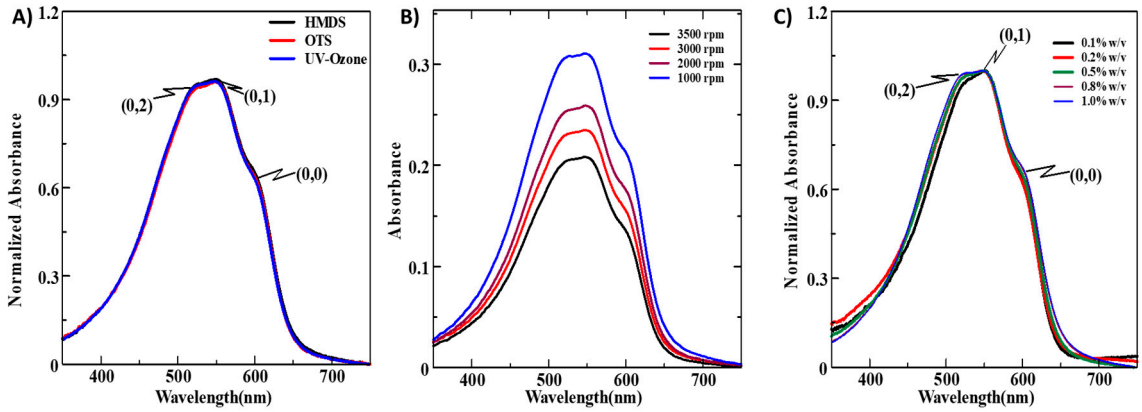

Figure 3. A) Normalized absorption spectra for spin-coated RR-P3HT thin films on glass substrate treated with different surface modifiers, B) absorption spectra at various spinning speeds and C) normalized absorption spectra of the films fabricated with varying polymer concentrations in chloroform.

For optimizing the effect of concentration, the concentration of the polymer solution was varied from 0.1 to 1% (w/v) while keeping the UV-ozone treated glass substrate and spinning speed of 3500 rpm as fixed parameters. It can be seen from the absorption spectra (Fig. S1D) that the thickness of the film increased on increasing the concentration of the solution and it was also validated that spin-coated films are isotropic since there was no color contrast in fabricated thin films upon rotating the polarizer from 0° to 90° (Fig. S1E). In the normalized absorption spectra (Figure 3C), the $A_{0\text{-}0}$, $A_{0\text{-}1}$, and $A_{0\text{-}2}$ transition peak values for the spin-coated thin film have been compared. These transition peaks refer to the absorption peaks and shoulders associated with the different electronic and vibrational transitions within the material. $A_{0\text{-}0}$ transition peak for RR-P3HT correlates to the intermolecular interactions, and presence/absence of defects. The $A_{0\text{-}1}$ transition peak is associated with the π-π^* transition. This transition is influenced by the degree of overlap between adjacent polymer chains, known as π-π stacking. The intensity and energy of the $A_{0\text{-}1}$ peak are sensitive to factors such as the degree of polymer crystallinity, chain orientation, and π-π interactions. $A_{0\text{-}2}$ correlates to the π-electron conjugation along the polymer backbone (intrachain interactions), reflecting the structural fluctuations or conformational changes along the polymer backbone [33,34]. The ratio $A_{0\text{-}0}/A_{0\text{-}1}$, that is coupling energy (W/E_P) (for Huang-Rhys Factor=1; W=Exciton bandwidth), provides information about the strength of electronic interchain coupling and degree of vibrational relaxation (E_P) across various polymer chains in thin film. A higher W/E_P is typically associated with an increase interchain ordering and crystalline domain arrangement, where electronic excitations can propagate with minimal energy dissipation through vibrational relaxation [35] (W/E_P for 0.8% and 1% solution is higher in comparison to other concentration of solution in their thin film state. This shows that 0.8% and 1% solution based thin films are highly ordered and crystalline with respect to the intermolecular interactions. On the other hand, ratio $A_{0\text{-}2}/A_{0\text{-}1}$, which corresponds to the intrachain coupling is lower for 0.1 and 0.2% concentration as compared to the other concentrations. A lower $A_{0\text{-}2}/A_{0\text{-}1}$ gives a lower exciton bandwidth resulting in ordered and narrowly distributed conjugation length. A concentration of 0.5%(w/v) for spin-coated thin films gives a good balance in attaining the coupling interactions for intramolecular as well as intermolecular ordering and crystallinity. Hence, 0.5% concentration was taken for the fabrication of OFETs for electrical characterizations.

3.2.2. Dip-Coated Thin Films

Dip-coating for thin film fabrication was developed to prepare large-area uniform thin films and for CPs it offers the advantage of utilizing their inherent molecular self-assembly owing to extended π-conjugation. At the same time, it is also advantageous over spin-coating in terms of material utilization. Parametric optimization such as the nature of the substrate surface, polymer concentration and lifting speeds has to be performed to control the film uniformity and morphology.

 doi:10.20944/preprints202404.1914.v1

Electronic absorption spectra dip-coated thin films prepared on differently surface-modified glass substrates are shown in the supporting information (Figure S2A) while keeping the polymer concentration and lifting speed of 1 % (w/v) and 20 μm/s, respectively. It was observed that dip-coated films have three distinct peaks $A_{0\text{-}0}$, $A_{0\text{-}1}$ and $A_{0\text{-}2}$ occurring at wavelengths of 600 nm, 550 nm and 510~520 nm, respectively, as shown in Figure 4(A). It has been widely reported that in RR-P3HT when the ratio of peak absorbances corresponding to $A_{0\text{-}0}/A_{0\text{-}1}$ is higher, it signifies enhanced crystallinity in the fabricated thin film and better molecular ordering. On the other hand, if the ratio of $A_{0\text{-}2}/A_{0\text{-}1}$ is pronounced it refers to interchain disorder [35,36]. It can be seen from the normalized absorption spectrum shown in Figure 4(A) that the ratio of $A_{0\text{-}0}/A_{0\text{-}1}$ is higher for OTS surface treatment followed by HMDS suggesting slightly better molecular ordering in the thin films fabricated on OTS. Despite this better ordering in the OTS-treated glass substrate, the film uniformity is inferior to that on the treated substrate, which can be seen from the photographic image shown in the supporting information (Fig. S2B). Moreover, dip-coated films could not be fabricated onto CYTOP-treated surfaces (Fig. S2B) due to the highly hydrophobic nature of CYTOP-treated substrates. Hence, for the dip coating technique, HMDS surface treatment would be the most suitable as it results in a homogenous and uniform film without seriously affecting the molecular ordering in the fabricated thin film.

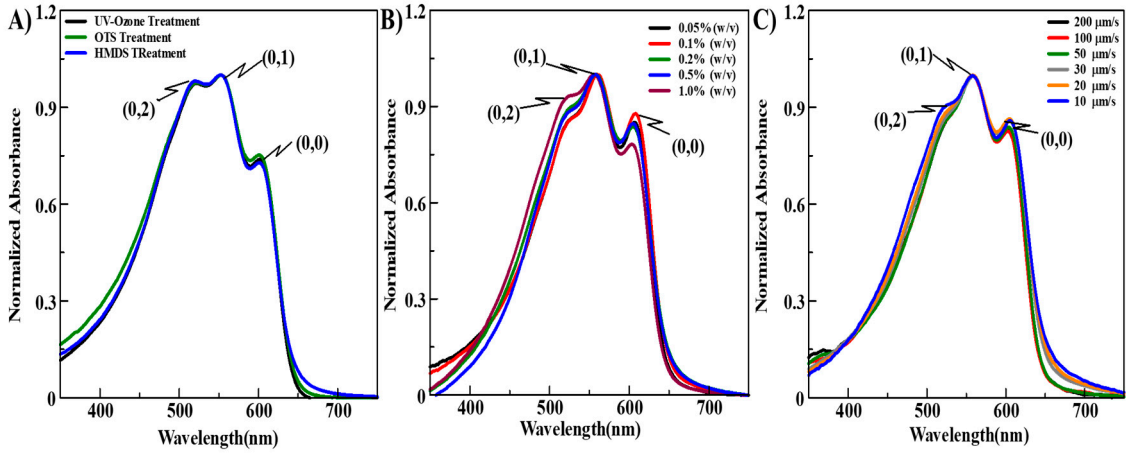

Figure 4. Normalized absorption spectra for dip-coated RR-P3HT thin films: A) on the differently surface-modified glass substrates, B) at different concentrations of the polymer and C) at various lifting speeds.

For the optimization of the effect of the concentration of CPs in dip-coating techniques, optical characterizations were performed on the glass substrates varying the concentration from 0.05 – 1% (w/v) and keeping the other variable parameters such as UV-ozone treated glass substrates at the lifting speed of 20μm/s. A perusal of Fig. S2(C) reveals that there was about 6 times increase in the thickness upon increasing the polymer concentration from 0.05% to 1.0% (w/v). Further, from normalized absorption spectra shown in Figure 4(B), confirm that the ratio $A_{0\text{-}0}/A_{0\text{-}1}$ decreases with the increasing polymer concentration and was highest for 0.1% concentration suggesting that the molecular ordering and crystallinity are best in this case. Moreover, when we compare the ratio of $A_{0\text{-}2}/A_{0\text{-}1}$ it can be concluded that 0.1% concentration exhibited the smallest molecular disordering, therefore, 0.1% concentration was found to be optimum and was used for the OFET device fabrication. Lifting speed during dip-coating is one of the most important parameters, which not only controls the thickness but also the quality (uniformity and morphology) of the fabricated thin films. Optimization of lifting speed in the dip-coating was performed by varying the lifting speed from 10 – 200 μm/s, keeping the other variable parameters such as the polymer concentration and nature of substrate to 0.2% (w/v) and UV ozone-treated glass substrate, respectively, to be fixed and results are shown in the Fig S2D. It can be seen from this figure shown in the supporting information that by decreasing the lifting speed from 10 μm/s to 200 μm/s, there was >10 times increase in film thickness (peak absorbance). At the same time, normalized absorption spectra shown in Figure 4(C) reveal that

 doi:10.20944/preprints202404.1914.v1

the ratio of $A_{0\text{-}0}/A_{0\text{-}1}$ peak for 20 μm/s and 10 μm/s lifting speed is almost similar pointing towards more ordered and crystalline film as compared to other lifting speeds. However, the films prepared at 10 μm/s speed were too thin film and non-uniform, therefore, 20 μm/s was found to be optimum for the device fabrication. Moreover, it was observed that dip-coated thin films are isotropic and non-oriented owing to the same color of the film (no contrast) under the parallel and perpendicular polarizer (Figure S2E, supporting information).

3.2.3. UFTM Fabricated Thin Films

The uniqueness of UFTM lies in the fact that we can not only fabricate large area and uniform thin films but also, they are anisotropic or oriented. At the same time, least material wastage and multilayer film fabrication by solution-based approach are its added advantages. The extent of the molecular orientation under UFTM can be controlled by controlling the film fabrication parameters like polymer concentration, temperature and viscosity of the liquid substrate [37]. It has been reported by our group previously that for RR-P3HT, a liquid substrate consisting of EG and GL in a 3:1 ratio gives the highest orientation, which has been used for the present work for the optimization of UFTM-processed thin films in this present work. To study the impact of surface treatment on UFTM-processed thin films, thin films were fabricated onto the HMDS, OTS, UV-Ozone and CYTOP-treated glass substrates keeping the other parameters like EG:GL (3:1) liquid substrate and 4 % of the polymer concentration fixed. The uniformity of the film and the presence of orientation can be clearly seen in the photographic images taken in the absence and presence of polarizer film (see Fig. S3A and S3B for supporting information) [38]. Polarized electronic absorption spectra were measured for UFTM-processed thin films fabricated on differently surface-modified glass substrates, which are shown in Figure 5(A). Optical anisotropy in terms of the optical dichroic ratio (DR) was calculated from the polarized absorption spectra and shown in Table 1. It can be seen from this figure and table nature of the surface treatment does not seriously affect the orientation of RR-P3HT, which was slightly better on CYTOP-modified glass substrate with a DR of 4.3. A perusal of the polarized absorption spectra reveals that in thin films of RR-P3HT fabricated by UFTM, there is a clear presence of absorption peaks around 550 nm associated with $A_{0\text{-}1}$ along with vibronic shoulders associated with $A_{0\text{-}0}$, and $A_{0\text{-}2}$. The pronounced absorption intensity for $A_{0\text{-}1}$ peak as compared to $A_{0\text{-}0}$ shoulder corroborates that UFTM-processed films are more crystalline and ordered owing to enhanced inter-chain interactions. From the normalized absorption spectra (Figure S3C, Supporting Information) it can be observed that the ratio $A_{0\text{-}0}/A_{0\text{-}1}$ associated with excitonic coupling energy (W) is almost similar and higher in the case of CYTOP and HMDS surface treatments pointing to more ordered and crystalline film as compared to UV-Ozone and OTS treated substrates. However, the transition peak $A_{0\text{-}2}$ is more dominant in the case of HMDS-treated substrate in comparison to CYTOP. Higher DR and better film quality make CYTOP, one of the most suitable surface treatments for UFTM, this can be due to the higher hydrophobicity of CYTOP, which aids in easily casting the solid film from a viscous liquid substrate.

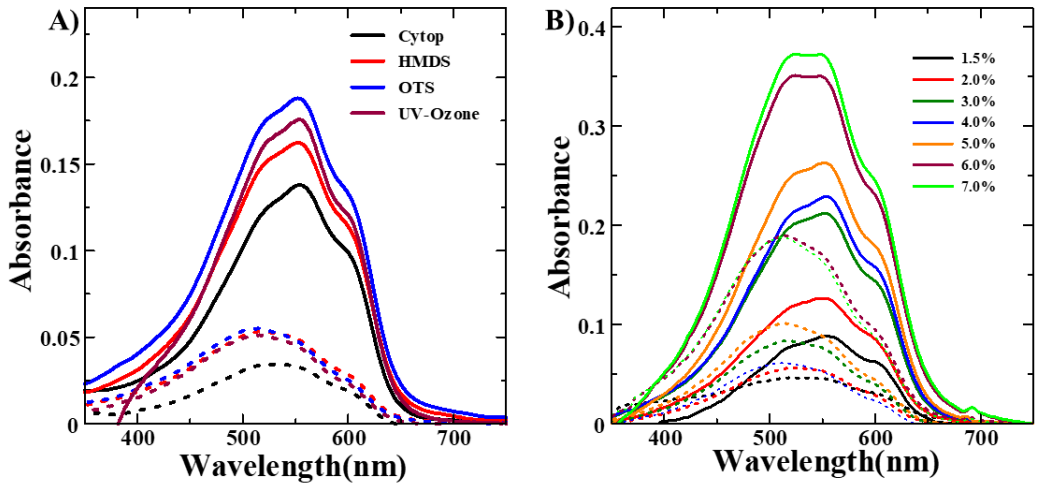

 doi:10.20944/preprints202404.1914.v1

Figure 5. Polarized electronic absorption spectra for UFTM-processed RR-P3HT thin films: A) on various surface treatments and B) at different concentrations. Solid and dotted lines represent spectra taken under parallel and perpendicular polarization.

Table 1. Effect of surface modification of glass and polymer concentration on the optical anisotropy of the UFTM processed thin films.

Polymer Conc. (w/v)	Surface Modifiers/Dichroic Ratio			
	UV-Ozone	HMDS	OTS	CYTOP
1.5%	1.8			
2.0%	2.5			
3.0%	3.1			
4.0%	4.2	4.1	4.0	4.3
5.0%	3.5			
6.0%	2.3			
7.0%	2.1			

The concentration of the polymer solution under UFTM plays a dominant role in not only controlling the film thickness but also molecular ordering and orientation by controlling the spreading speed of the of polymer solution on the orthogonal viscous liquid substrate. In this present work, the effect of polymer concentration on the nature of the fabricated thin film was estimated by varying the concentration of RR-P3HT solution from 1.5 to 7% (w/v) while keeping other variables like EG:GL (3:1) liquid substrate and UV-Ozone treated glass substrate as fixed parameters. Polarized absorption spectra recorded for oriented thin films fabricated using varying polymer concentrations are shown in Figure 5(B) along with the summarization of calculated optical anisotropy in terms of optical DR in Table 1. It can be seen from this figure and table that there is about 4 times increase in the thickness of UFTM-processed thin films upon increasing the polymer concentration from 1.5 % to 7.0 %, which is almost linear.

Moreover, the dichroic ratio calculated for various concentrations as summarized in Table 1 indicates a gradual increase followed by a decrease in DR, with a maximum DR at the 4% polymer concentration suggesting the presence of maximum orientation. From the normalized spectra in Figure S3D of supporting information, it was observed that the ratio of vibronic peak $A_{0\text{-}0}/A_{0\text{-}1}$ for lower concentrations is better in comparison to higher concentrations of films, which also have dominant $A_{0\text{-}2}$ peaks. Moreover, there is an observed redshift for lower concentrations of CP solution indicating that lower concentration films were more ordered and crystalline. However, considering the better DR, good film quality and optimum thickness for ease of fabrication and uniformity, a concentration of 4% was found to be optimum and was used for OFET fabrication.

3.3. Microstructural Characterization

To explore the crystallinity and macromolecular orientation, in-plane GIXD and out-of-plane XRD measurements were performed for the fabricated thin films of the RR-P3HT (Figure 6). From the out-of-plane XRD analysis of RR-P3HT films fabricated via UFTM and dip coating as shown in Figure 6(A), a sharp diffraction peak corresponding to the lamellar stacking of the alkyl side chains up to the 3rd order, at θ values of 5.5°, 11°, and 16°, which corresponds to the (hkl) value of (100), (200), and (300), respectively, was evident. In addition to this, the thin film of UFTM also demonstrated a 2θ value of 23.5° corresponding to (010), with a plane separation value of 3.9 Å (b or c-axis, lattice constant), and lattice separation at 2θ of 5.5° is 16 Å corresponding to the lattice constant of a-axis of RR-P3HT [39,40]. From this, analysis it can be stated that in RR-P3HT, the polymer chain exhibits an orientation close to parallel alignment with the substrate, while the individual thiophene rings within the polymer structure are oriented perpendicular to the substrate surface; these observations are in close relation with the previously reported works [39,40]. Moreover, the spin-coated thin film exhibits a comparatively weak (100) peak of the second order, indicating that the films made through dip coating and UFTM are more crystalline. Also, it is depicted from these diffraction peaks that RR-P3HT films fabricated via UFTM are more crystalline than its contrary dip

 doi:10.20944/preprints202404.1914.v1

coating film, as its (100) peak is not only weaker but also its full width at half maximum is relatively narrow. Further, from the analysis of in-plane GIXD of RR-P3HT films shown in Figure 6(B), it was clear that the films prepared using UFTM and dip coating did not display any diffraction peaks linked to alkyl side chains, as it only showcased a diffraction peak, with an (hkl) value of (010), at ~23.3° in both the cases, which reveals that all crystallites are oriented edge-on [24]. Apart from this, the spin-coated film of the CP exhibited no (010) diffraction peaks, because this film has its crystallite fractions, oriented face-on [41]. Thus, the prepared RR-P3HT films by dip coating and UFTM are more ordered and crystalline than spin-coated films, which is attributed to the results of the in-plane and out-of-plane XRD profiles of the films. While comparing the results of this study with other pre-existing literature, it was observed that Yang et al. [42] reported P3HT/CHCl3 films, mostly have face-on crystal orientation that is highly favorable toward the vertical charge transport for devices like diodes and solar cells. In another study by De Long Champ et al. [43] it was reported that spin-coated RR-P3HT/$CHCl_3$ thin films at a spinning speed of ~2000 rpm was preferentially face-on oriented. Hence, from this analysis, it was revealed that the spin-coated films are in majority face-on and UFTM and dip coating films were oriented edge-on.

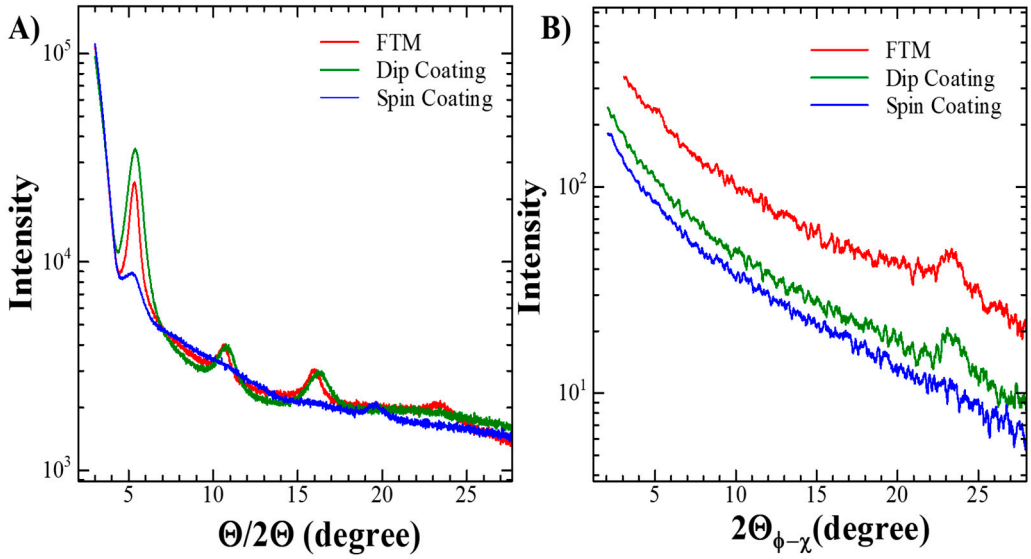

Figure 6. A) Out-of-plane XRD and B) In-plane GIXD profiles for the thin films fabricated with UFTM, dip coating and spin coating.

3.4. Electrical Characterization

After the initial studies to investigate the effect of crystallinity and molecular orientation of CP thin films of RR-P3HTs fabricated using UFTM, dip-coating, and spin-coating; OFETs were fabricated in the BGTC device architecture as shown in Figure 1(B), for investigating anisotropic charge transport. In the previous reports by our group, it has already been reported that thin film fabrication by UFTM is oriented edge-on, which facilitates the facile in-plane charge transport [44,45]. In addition to this, Xue et al. [46] reported that RR-P3HT dip-coated films are edge-on oriented. In the case of spin-coated RR-P3HT film as a semiconductor demonstrates face-on orientation or mixed orientation [47,48]. In this study for OFET fabrication, initially, Si/SiO_2 substrates were surface treated with HMDS to make the substrate's surface hydrophobic before thin film fabrication using RR-P3HT because the polymer under investigation is hydrophobic. Then, the thin film was fabricated by using optimum concentrations of RR-P3HT solution for different thin film fabrication techniques, which are 0.5%, 0.1%, and 4% (w/v) for spin-coating, dip-coating, and UFTM, respectively. The SiO_2 gate oxide dielectric thickness was kept constant at 300 nm. Finally, from the output and transfer characteristics obtained by the I–V (current–voltage) characteristics shown in Figure 7, it was evident that the output curves depicted by Figure 7(i) demonstrated p-type semiconducting behavior, as evident from the modulation of channel current upon application of the differential negative bias voltage. In addition, Eq. (2) was used to obtain the field effect mobility (μ) from the transfer curves

 doi:10.20944/preprints202404.1914.v1

shown in Figure 7(ii) in the saturation region; where, μ, C_i, W, and L stand for saturated mobility, areal capacitance, channel width, and channel length, respectively.

$$I_{Ds} = \frac{\mu C_i W}{2L}(V_{GS} - V_{DS})^2 \quad \text{Eq. (2)}$$

Source-drain current (I_{DS}), gate voltage (V_{GS}), and drain-source voltage (V_{DS}) are the corresponding terms. In the saturated region, the slope of the $|I_{DS}|^{1/2}$ versus V_{GS} plot was used to calculate the μ, while the ratio of the on-to-off current in the transfer characteristic was used to calculate the on-off ratio [11]. Further, for the fabrication of OFETs by UFTM-processed oriented thin films, parallel and perpendicular OFETs were also fabricated by aligning the source and drain electrodes of the channel towards both the parallel and perpendicular to the orientation direction to study anisotropic charge transport. The output and transfer characteristics of the fabricated OFETs by spin coating (Figure 7A), dip-coating (Figure 7B), and UFTM (Figure 7C & D) are presented in Figure 7.

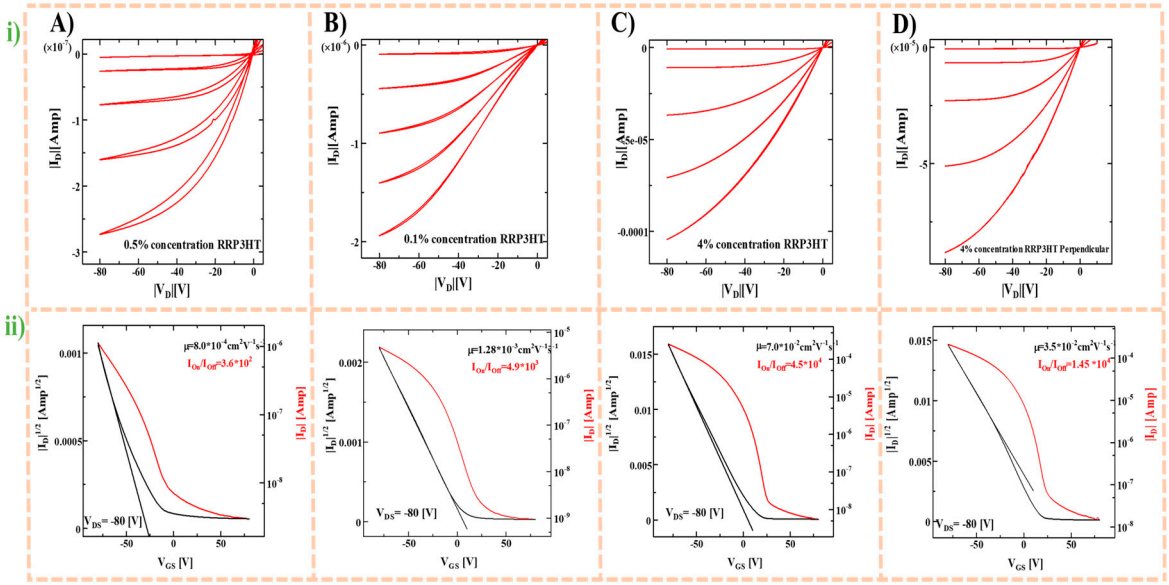

Figure 7. (i) Output and (ii) Transfer characteristics of A) spin-coated, B) Dip-coated, C) UFTM-processed parallel, and D) UFTM-processed perpendicular OFETs.

The calculated value of μ and on/off ratio from the transfer characteristics for the fabricated OFETs by utilizing RR-P3HT thin films prepared by spin-coating, dip-coating, and UFTM are summarized in Table 2.

Table 2. Electrical parameters of OFETs fabricated using RR-P3HT thin films fabricated by various techniques such as spin-coating, dip-coating and UFTM.

Fabrication Techniques	Concentration (w/v)	Thickness (nm)	Carrier mobility ($cm^2V^{-1}s^{-1}$)	On-off Ratio
Spin-coating	0.5 %	34	8.0×10^{-4}	3.6×10^2
Dip-coating	0.1 %	29	1.3×10^{-3}	4.9×10^3
UFTM	4.0 %	23	7.0×10^{-2}	4.5×10^4

A perusal of Figure 7 and Table 1 reveals that in OFETs fabricated using spin-coated RR-P3HT, there was a significant leakage in current at zero gate bias, which resulted in an extremely low on-off ratio of 3.6×10^2 and μ of 8.0×10^{-4} $cm^2V^{-1}s^{-1}$. On the other hand, μ estimated for the dip-coat fabricated OFET, there was about two times improvement in the carrier mobility (1.3×10^{-3} $cm^2V^{-1}s^{-1}$) while an order of magnitude enhancement in the on/off ratio (4.9×10^3) as compared to its spin-coated OFETs device counterparts. Interestingly, OFETs that used parallel-oriented RR-P3HT thin films showed significantly improved charge carrier transport, with μ and on/off ratios of 7.0×10^{-2} $cm^2V^{-1}s^{-1}$and 4.5×10^4, respectively. Apart from this, OFETs that were fabricated using oriented thin films by UFTM

 doi:10.20944/preprints202404.1914.v1

demonstrated electrical anisotropy ($\mu^{\parallel}/\mu^{\perp}$) of 2. When compared to their UFTM and dip-coating processed device counterparts, the presence of face-on fractions in spin-coated thin films with alkyl chains positioned in the substrate plane results in reduced in-plane charge transport and impeded OFET performance. In the dip-coating technique fabricated OFETs exhibited lower mobility than the UFTM-processed device, due to the absence of orientation and the presence of relatively higher disordered polymer domains in the film. OFETs fabricated using UFTM showed an enhanced planar charge transport, with an average μ that was more than two orders of magnitude higher (7.0×10^{-2} $cm^2V^{-1}s^{-1}$) than that of OFETs spin-coated thin films (8×10^{-4} $cm^2V^{-1}s^{-1}$). Enhanced molecular orientation and crystallinity resulted in a notable improvement in OFETs with an active layer made using UFTM that is nearly 10 times higher μ value compared to RR-P3HT films prepared by dip-coating and nearly 100 times higher by spin-coating. Since the crystallinity of dip-coated and UFTM-processed thin films are almost similar but about 50 enhancements in the carrier mobility of UFTM-processed thin films suggest that molecular orientation undoubtedly plays a dominant role as compared to crystallinity in controlling the charge transport.

5. Conclusions

In this study, thin films of the RR-P3HT have been fabricated using three different solution-processable thin film fabrication techniques, namely spin-coating, dip-coating, and UFTM. Initially, optimizing various parameters affecting the thin film properties was carried out in detail using optical and microstructural characterizations followed by the fabrication of OFETs. Thin films fabricated by UFTM were large-area, oriented, crystalline, and anisotropic. In contrast, spin-coated and dip-coated thin films were non-oriented and isotropic, but dip-coated films were more crystalline as compared to spin-coated films, which was confirmed by the electronic absorption spectra and XRD results. Moreover, various parameters affecting the quality of the thin film were studied in detail, such as surface treatment and it was found that a strongly hydrophobic surface was better for UFTM, whereas mild hydrophobicity of the surface ensured the best film quality in the case of spin-coating and dip-coating. Further, the XRD and GIXD results show that macromolecular chains in UFTM and dip-coated films were edge-on oriented facilitating better planar charge transport as compared to spin-coated films. Finally, OFETs were fabricated to analyze the implications of molecular orientation and crystallinity on device performance. Thus, the electrical parameters such as mobility verified that edge-on orientation and crystallinity enhance the device performance in OFETs fabricated by UFTM and dip-coating when compared to spin-coating. There was a notable enhancement (>10^2 times) in mobility for UFTM-processed thin films of RR-P3HT as compared to spin-coated device counterparts, which was attributed to the enhancement of crystallinity and the presence of the molecular orientation, Hence, this study underscores the promising prospects of utilizing UFTM and dip-coating for fabricating high-performance OFETs with enhanced charge mobility and on/off ratios compared to spin-coating.

Supplementary Materials: The following supporting information can be downloaded at the website of this paper posted on Preprints.org, Figure S1: Optimization and Optical characterizations of spin-coated films; Figure S2: Optimization and Optical characterizations of dip-coated films; Figure S3: Optimization and Optical characterizations of FTM-processed thin films

Author Contributions: Conceptualization, K.V.G and S.S.P.; methodology, K.V.G.; software, Y.A.; validation, S.S.P.; formal analysis, S.S. and S.S.P.; investigation, K.V.G. and H.R.; resources, S.S.P.; data curation, K.V.G.; writing—original draft preparation, K.V.G.; writing—review and editing, H.R. and K.R.B.S.; visualization, K.V.G. and S.S.P.; supervision, S.S.P.; project administration, S.S.P.; funding acquisition, S.S.P. All authors have read and agreed to the published version of the manuscript. All the authors reviewed the manuscript before submission.

Funding: This work did not receive any specific grant from funding agencies in the public, commercial, or not-for-profit sectors.

Data Availability Statement: Data will be made available on request.

 doi:10.20944/preprints202404.1914.v1

Acknowledgments: K.V.G. would like to express sincere thanks to the Japanese government's Ministry of Education, Science, Sports and Culture (MEXT) for providing scholarships for carrying out the present research.

Conflicts of Interest: The authors declare no conflicts of interest.

References

1. W. M. Arden, The International Technology Roadmap for Semiconductors—Perspectives and challenges for the next 15 years, Curr Opin Solid State Mater Sci 6 (2002) 371–377. https://doi.org/10.1016/S1359-0286(02)00116-X.
2. M.C. Petty, Molecular Electronics, John Wiley & Sons, Ltd., Chichester, UK, 2007. https://doi.org/10.1002/9780470723890.
3. M. Ikawa, T. Yamada, H. Matsui, H. Minemawari, J. Tsutsumi, Y. Horii, M. Chikamatsu, R. Azumi, R. Kumai, T. Hasegawa, Simple push coating of polymer thin-film transistors, Nat Commun 3 (2012) 1176. https://doi.org/10.1038/ncomms2190.
4. L. Sun, Y. Kurosawa, H. Ito, Y. Makishima, H. Kita, T. Yoshida, Y. Suzuri, Solution processing of alternating PDMS/SiOx multilayer for encapsulation of organic light emitting diodes, Org Electron 64 (2019) 176–180. https://doi.org/10.1016/j.orgel.2018.10.027.
5. A. Sandström, H.F. Dam, F.C. Krebs, L. Edman, Ambient fabrication of flexible and large-area organic light-emitting devices using slot-die coating, Nat Commun 3 (2012) 1002. https://doi.org/10.1038/ncomms2002.
6. L. Yuan, S. Liu, W. Chen, F. Fan, G. Liu, Organic Memory and Memristors: From Mechanisms, Materials to Devices, Adv Electron Mater 7 (2021). https://doi.org/10.1002/aelm.202100432.
7. A. Marrocchi, D. Lanari, A. Facchetti, L. Vaccaro, Poly(3-hexylthiophene): synthetic methodologies and properties in bulk heterojunction solar cells, Energy Environ Sci 5 (2012) 8457. https://doi.org/10.1039/c2ee22129b.
8. J. Xu, H.-C. Wu, C. Zhu, A. Ehrlich, L. Shaw, M. Nikolka, S. Wang, F. Molina-Lopez, X. Gu, S. Luo, D. Zhou, Y.-H. Kim, G.-J.N. Wang, K. Gu, V.R. Feig, S. Chen, Y. Kim, T. Katsumata, Y.-Q. Zheng, H. Yan, J.W. Chung, J. Lopez, B. Murmann, Z. Bao, Multi-scale ordering in highly stretchable polymer semiconducting films, Nat Mater 18 (2019) 594–601. https://doi.org/10.1038/s41563-019-0340-5.
9. J.Y. Oh, S. Rondeau-Gagné, Y.-C. Chiu, A. Chortos, F. Lissel, G.-J.N. Wang, B.C. Schroeder, T. Kurosawa, J. Lopez, T. Katsumata, J. Xu, C. Zhu, X. Gu, W.-G. Bae, Y. Kim, L. Jin, J.W. Chung, J.B.-H. Tok, Z. Bao, Intrinsically stretchable and healable semiconducting polymer for organic transistors, Nature 539 (2016) 411–415. https://doi.org/10.1038/nature20102.
10. H. Sirringhaus, 25th Anniversary Article: Organic Field-Effect Transistors: The Path Beyond Amorphous Silicon, Advanced Materials 26 (2014) 1319–1335. https://doi.org/10.1002/adma.201304346.
11. H. Sirringhaus, Device Physics of Solution-Processed Organic Field-Effect Transistors, Advanced Materials 17 (2005) 2411–2425. https://doi.org/10.1002/adma.200501152.
12. J.L. Mi, X.B. Zhao, T.J. Zhu, J.P. Tu, Improved thermoelectric figure of merit in n-type CoSb3 based nanocomposites, Appl Phys Lett 91 (2007). https://doi.org/10.1063/1.2803847.
13. J.-F. Chang, B. Sun, D.W. Breiby, M.M. Nielsen, T.I. Sölling, M. Giles, I. McCulloch, H. Sirringhaus, Enhanced Mobility of Poly(3-hexylthiophene) Transistors by Spin-Coating from High-Boiling-Point Solvents, Chemistry of Materials 16 (2004) 4772–4776. https://doi.org/10.1021/cm049617w.
14. J. Noh, S. Jeong, J.-Y. Lee, Ultrafast formation of air-processable and high-quality polymer films on an aqueous substrate, Nat Commun 7 (2016) 12374. https://doi.org/10.1038/ncomms12374.
15. Y. Yabuuchi, G. Uzurano, M. Nakatani, A. Fujii, M. Ozaki, Uniaxial orientation of poly(3-hexylthiophene) thin films fabricated by the bar-coating method, Jpn J Appl Phys 58 (2019) SBBG04. https://doi.org/10.7567/1347-4065/aafb5d.
16. M. Brinkmann, L. Hartmann, L. Biniek, K. Tremel, N. Kayunkid, Orienting Semi-Conducting π-Conjugated Polymers, Macromol Rapid Commun 35 (2014) 9–26. https://doi.org/10.1002/marc.201300712.
17. S. Nagamatsu, W. Takashima, K. Kaneto, Y. Yoshida, N. Tanigaki, K. Yase, K. Omote, Backbone Arrangement in "Friction-Transferred" Regioregular Poly(3-alkylthiophene)s, Macromolecules 36 (2003) 5252–5257. https://doi.org/10.1021/ma025887t.
18. A. Salleo, R.J. Kline, D.M. DeLongchamp, M.L. Chabinyc, Microstructural Characterization and Charge Transport in Thin Films of Conjugated Polymers, Advanced Materials 22 (2010) 3812–3838. https://doi.org/10.1002/adma.200903712.
19. R. Noriega, J. Rivnay, K. Vandewal, F.P. V. Koch, N. Stingelin, P. Smith, M.F. Toney, A. Salleo, A general relationship between disorder, aggregation and charge transport in conjugated polymers, Nat Mater 12 (2013) 1038–1044. https://doi.org/10.1038/nmat3722.
20. J. Puetz, M.A. Aegerter, Dip Coating Technique, in: Sol-Gel Technologies for Glass Producers and Users, Springer US, Boston, MA, 2004: pp. 37–48. https://doi.org/10.1007/978-0-387-88953-5_3.

21. H. Rai, K. Vivek Gaurav, S. Pradhan, M. Desu, S. Sharma, S. Nagamatsu, S.S. Pandey, Vertical Distribution of Molecular Orientation and Its Implication on Charge Transport in Floating Films of Conjugated Polymers, Physica Status Solidi (a) 220 (2023). https://doi.org/10.1002/pssa.202300236.
22. N. Kumari, S. Sharma, S. Nagamatsu, S.S. Pandey, Orientation of Semiconducting Polymers via Swift Printing and Drawing Techniques for High Performance Organic Electronic Devices, in: 2020 27th International Workshop on Active-Matrix Flatpanel Displays and Devices (AM-FPD), IEEE, 2020: pp. 67–70. https://doi.org/10.23919/AM-FPD49417.2020.9224472.
23. M. Pandey, N. Kumari, S. Nagamatsu, S.S. Pandey, Recent advances in the orientation of conjugated polymers for organic field-effect transistors, J Mater Chem C Mater 7 (2019) 13323–13351. https://doi.org/10.1039/C9TC04397G.
24. M. Pandey, A. Gowda, S. Nagamatsu, S. Kumar, W. Takashima, S. Hayase, S.S. Pandey, Rapid Formation and Macroscopic Self-Assembly of Liquid-Crystalline, High-Mobility, Semiconducting Thienothiophene, Adv Mater Interfaces 5 (2018) 1700875. https://doi.org/10.1002/admi.201700875.
25. M. Pandey, S. Nagamatsu, S.S. Pandey, S. Hayase, W. Takashima, Orientation Characteristics of Non-regiocontrolled Poly (3-hexyl-thiophene) Film by FTM on Various Liquid Substrates, J Phys Conf Ser 704 (2016) 012005. https://doi.org/10.1088/1742-6596/704/1/012005.
26. Appendix C: Contact Angle Goniometry, in: Surface Design: Applications in Bioscience and Nanotechnology, Wiley, 2009: pp. 471–473. https://doi.org/10.1002/9783527628599.app3.
27. H.-W. Zan, C.-W. Chou, Effect of Surface Energy on Pentacene Thin-Film Growth and Organic Thin Film Transistor Characteristics, Jpn J Appl Phys 48 (2009) 031501. https://doi.org/10.1143/JJAP.48.031501.
28. S.C. Lim, S.H. Kim, J.H. Lee, M.K. Kim, D.J. Kim, T. Zyung, Surface-treatment effects on organic thin-film transistors, Synth Met 148 (2005) 75–79. https://doi.org/10.1016/j.synthmet.2004.08.034.
29. Jon Griffin, Emma Spooner, Hadi Hassan, Spin Coating: Complete Guide to Theory and Techniques, Ossila (n.d.). https://www.ossila.com/pages/spin-coating#:~:text=As%20mentioned%20above%2C%20spin%20coating,at%20the%20expense%20of%20consistency (accessed February 20, 2024).
30. R. Förch, H. Schönherr, A.T.A. Jenkins, eds., Surface Design: Applications in Bioscience and Nanotechnology, Wiley, 2009. https://doi.org/10.1002/9783527628599.
31. F.C. Spano, Erratum: "Modeling disorder in polymer aggregates: The optical spectroscopy of regioregular poly(3-hexylthiophene) thin films" [J. Chem. Phys. 122, 234701 (2005)], J Chem Phys 126 (2007). https://doi.org/10.1063/1.2721549.
32. F.C. Spano, C. Silva, H- and J-Aggregate Behavior in Polymeric Semiconductors, Annu Rev Phys Chem 65 (2014) 477–500. https://doi.org/10.1146/annurev-physchem-040513-103639.
33. M. Baghgar, J.A. Labastide, F. Bokel, R.C. Hayward, M.D. Barnes, Effect of Polymer Chain Folding on the Transition from H- to J-Aggregate Behavior in P3HT Nanofibers, The Journal of Physical Chemistry C 118 (2014) 2229–2235. https://doi.org/10.1021/jp411668g.
34. J. Clark, J.-F. Chang, F.C. Spano, R.H. Friend, C. Silva, Determining exciton bandwidth and film microstructure in polythiophene films using linear absorption spectroscopy, Appl Phys Lett 94 (2009). https://doi.org/10.1063/1.3110904.
35. F.C. Spano, Modeling disorder in polymer aggregates: The optical spectroscopy of regioregular poly(3-hexylthiophene) thin films, J Chem Phys 122 (2005). https://doi.org/10.1063/1.1914768.
36. G. Wang, T. Hirasa, D. Moses, A.J. Heeger, Fabrication of regioregular poly(3-hexylthiophene) field-effect transistors by dip-coating, Synth Met 146 (2004) 127–132. https://doi.org/10.1016/j.synthmet.2004.06.026.
37. S. Sharma, A.K. Vats, L. Tang, F. Kaishan, J. Toyoda, S. Nagamatsu, Y. Ando, M. Tamagawa, H. Tanaka, M. Pandey, S.S. Pandey, High field-effect mobility in oriented thin films of D-A type semiconducting polymers by engineering stable interfacial system, Chemical Engineering Journal 469 (2023) 143932. https://doi.org/10.1016/j.cej.2023.143932.
38. M. Pandey, Y. Sugita, J. Toyoda, S. Katao, R. Abe, Y. Cho, H. Benten, M. Nakamura, Unidirectionally Aligned Donor–Acceptor Semiconducting Polymers in Floating Films for High-Performance Unipolar n -Channel Organic Transistors, Adv Electron Mater 9 (2023). https://doi.org/10.1002/aelm.202201043.
39. R.G.S. Goh, E.R. Waclawik, N. Motta, J.M. Bell, Influence of dispersed carbon nanotubes on the optical and structural properties of a conjugated polymer, in: J.-C. Chiao, A.S. Dzurak, C. Jagadish, D. V. Thiel (Eds.), 2005: p. 60370Z. https://doi.org/10.1117/12.638671.
40. K. Sugiyama, T. Kojima, H. Fukuda, H. Yashiro, T. Matsuura, Y. Shimoyama, ESR and X-ray diffraction studies on thin films of poly-3-hexylthiophene: Molecular orientation and magnetic interactions, Thin Solid Films 516 (2008) 2691–2694. https://doi.org/10.1016/j.tsf.2007.04.067.
41. N. Kumari, M. Pandey, S. Nagamatsu, M. Nakamura, S.S. Pandey, Investigation and Control of Charge Transport Anisotropy in Highly Oriented Friction-Transferred Polythiophene Thin Films, ACS Appl Mater Interfaces 12 (2020) 11876–11883. https://doi.org/10.1021/acsami.9b23345.
42. H. Yang, S.W. LeFevre, C.Y. Ryu, Z. Bao, Solubility-driven thin film structures of regioregular poly(3-hexyl thiophene) using volatile solvents, Appl Phys Lett 90 (2007). https://doi.org/10.1063/1.2734387.

43. D.M. DeLongchamp, B.M. Vogel, Y. Jung, M.C. Gurau, C.A. Richter, O.A. Kirillov, J. Obrzut, D.A. Fischer, S. Sambasivan, L.J. Richter, E.K. Lin, Variations in Semiconducting Polymer Microstructure and Hole Mobility with Spin-Coating Speed, Chemistry of Materials 17 (2005) 5610–5612. https://doi.org/10.1021/cm0513637.
44. S. Sharma, N. Kumari, S. Nagamatsu, M. Nakamura, S.S. Pandey, Bistable Resistive Memory Switches fabricated by Floating Thin Films of Conjugated Polymers, Materials Today Electronics 4 (2023) 100043. https://doi.org/10.1016/j.mtelec.2023.100043.
45. H. Rai, K. Vivek Gaurav, S. Pradhan, M. Desu, S. Sharma, S. Nagamatsu, S.S. Pandey, Vertical Distribution of Molecular Orientation and Its Implication on Charge Transport in Floating Films of Conjugated Polymers, Physica Status Solidi (a) (2023). https://doi.org/10.1002/pssa.202300236.
46. L. Xue, X. Gao, K. Zhao, J. Liu, X. Yu, Y. Han, The formation of different structures of poly(3-hexylthiophene) film on a patterned substrate by dip coating from aged solution, Nanotechnology 21 (2010) 145303. https://doi.org/10.1088/0957-4484/21/14/145303.
47. N. Yadav, K. Bhargava, N. Kumari, S.S. Pandey, V. Singh, Comparative analysis of metal diffusion effects in polymer films coated with spin coating and floating film transfer techniques, Synth Met 264 (2020) 116378. https://doi.org/10.1016/j.synthmet.2020.116378.
48. N. Kumari, M. Pandey, K. Hamada, D. Hirotani, S. Nagamatsu, S. Hayase, S.S. Pandey, Role of device architecture and AlOX interlayer in organic Schottky diodes and their interpretation by analytical modeling, J Appl Phys 126 (2019). https://doi.org/10.1063/1.5109083.